Hard Two-Body Photodisintegration of ^{3}He

I. Pomerantz,[46,45] Y. Ilieva,[44] R. Gilman,[41,48] D. W. Higinbotham,[48] E. Piasetzky,[45] S. Strauch,[44] K. P. Adhikari,[38] M. Aghasyan,[22] K. Allada,[30] M. J. Amaryan,[38] S. Anefalos Pereira,[22] M. Anghinolfi,[23] H. Baghdasaryan,[52] J. Ball,[7] N. A. Baltzell,[1] M. Battaglieri,[23] V. Batourine,[48] A. Beck,[35] S. Beck,[35] I. Bedlinskiy,[27] B. L. Berman,[17,*] A. S. Biselli,[13,39] W. Boeglin,[14] J. Bono,[14] C. Bookwalter,[15] S. Boiarinov,[48,27] W. J. Briscoe,[17] W. K. Brooks,[50,48] N. Bubis,[45] V. Burkert,[48] A. Camsonne,[48] M. Canan,[38] D. S. Carman,[48] A. Celentano,[23] S. Chandavar,[37] G. Charles,[7] K. Chirapatpimol,[52] E. Cisbani,[25] P. L. Cole,[19,48] M. Contalbrigo,[21] V. Crede,[15] F. Cusanno,[25] A. D'Angelo,[24,40] A. Daniel,[37] N. Dashyan,[54] C. W. de Jager,[48] R. De Vita,[23] E. De Sanctis,[22] A. Deur,[48] C. Djalali,[44] G. E. Dodge,[38] D. Doughty,[8,48] R. Dupre,[7] C. Dutta,[30] H. Egiyan,[48,53] A. El Alaoui,[1] L. El Fassi,[1] P. Eugenio,[15] G. Fedotov,[44] S. Fegan,[51] J. A. Fleming,[12] A. Fradi,[26] F. Garibaldi,[25] O. Geagla,[52] N. Gevorgyan,[54] K. L. Giovanetti,[28] F. X. Girod,[48] J. Glister,[42,10] J. T. Goetz,[3] W. Gohn,[9] E. Golovatch,[43,23] R. W. Gothe,[44] K. A. Griffioen,[53] B. Guegan,[26] M. Guidal,[26] L. Guo,[14] K. Hafidi,[1] H. Hakobyan,[50,54] N. Harrison,[9] D. Heddle,[8,48] K. Hicks,[37] D. Ho,[5] M. Holtrop,[34] C. E. Hyde,[38] D. G. Ireland,[51] B. S. Ishkhanov,[43] E. L. Isupov,[43] X. Jiang,[41] H. S. Jo,[26] K. Joo,[9,52] A. T. Katramatou,[29] D. Keller,[52] M. Khandaker,[36] P. Khetarpal,[14] E. Khrosinkova,[29] A. Kim,[31] W. Kim,[31] F. J. Klein,[6] S. Koirala,[38] A. Kubarovsky,[39,43] V. Kubarovsky,[48] S. V. Kuleshov,[50,27] N. D. Kvaltine,[52] B. Lee,[29] J. J. LeRose,[48] S. Lewis,[51] R. Lindgren,[52] K. Livingston,[51] H. Y. Lu,[5] I. J. D. MacGregor,[51] Y. Mao,[44] D. Martinez,[19] M. Mayer,[38] E. McCullough,[42] B. McKinnon,[51] D. Meekins,[48] C. A. Meyer,[5] R. Michaels,[48] T. Mineeva,[9] M. Mirazita,[22] B. Moffit,[53] V. Mokeev,[48,43,†] R. A. Montgomery,[51] H. Moutarde,[7] E. Munevar,[48] C. Munoz Camacho,[26] P. Nadel-Turonski,[48] R. Nasseripour,[28,14] C. S. Nepali,[38] S. Niccolai,[26] G. Niculescu,[28,37] I. Niculescu,[28,17] M. Osipenko,[23] A. I. Ostrovidov,[15] L. L. Pappalardo,[21] R. Paremuzyan,[54,‡] K. Park,[48,31] S. Park,[15] G. G. Petratos,[29] E. Phelps,[44] S. Pisano,[22] O. Pogorelko,[27] S. Pozdniakov,[27] S. Procureur,[7] D. Protopopescu,[51] A. J. R. Puckett,[48] X. Qian,[11] Y. Qiang,[33] G. Ricco,[16,§] D. Rimal,[14] M. Ripani,[23] B. G. Ritchie,[2] I. Rodriguez,[14] G. Ron,[18] G. Rosner,[51] P. Rossi,[22] F. Sabatié,[7] A. Saha,[48,*] M. S. Saini,[15] A. J. Sarty,[42] B. Sawatzky,[52,47] N. A. Saylor,[39] D. Schott,[17] E. Schulte,[41] R. A. Schumacher,[5] E. Seder,[9] H. Seraydaryan,[38] R. Shneor,[45] G. D. Smith,[51] D. Sokhan,[26] N. Sparveris,[33,47] S. S. Stepanyan,[31] S. Stepanyan,[48] P. Stoler,[39] R. Subedi,[29] V. Sulkosky,[48] M. Taiuti,[16,§] W. Tang,[37] C. E. Taylor,[19] S. Tkachenko,[52] M. Ungaro,[48,39] B. Vernarsky,[5] M. F. Vineyard,[49] H. Voskanyan,[54] E. Voutier,[32] N. K. Walford,[6] Y. Wang,[20] D. P. Watts,[12] L. B. Weinstein,[38] D. P. Weygand,[48] B. Wojtsekhowski,[48] M. H. Wood,[4] X. Yan,[29] H. Yao,[47] N. Zachariou,[44] X. Zhan,[33] J. Zhang,[48] Z. W. Zhao,[52] X. Zheng,[52] and I. Zonta[24,‖]

(CLAS and Hall-A Collaborations)

[1]*Argonne National Laboratory, Argonne, Illinois 60439, USA*
[2]*Arizona State University, Tempe, Arizona 85287-1504, USA*
[3]*University of California at Los Angeles, Los Angeles, California 90095-1547, USA*
[4]*Canisius College, Buffalo, New York 14208, USA*
[5]*Carnegie Mellon University, Pittsburgh, Pennsylvania 15213, USA*
[6]*Catholic University of America, Washington, D.C. 20064, USA*
[7]*CEA, Centre de Saclay, Irfu/Service de Physique Nucléaire, 91191 Gif-sur-Yvette, France*
[8]*Christopher Newport University, Newport News, Virginia 23606, USA*
[9]*University of Connecticut, Storrs, Connecticut 06269, USA*
[10]*Dalhousie University, Halifax, Nova Scotia B3H 3J5, Canada*
[11]*Duke University, Durham, North Carolina 27708, USA*
[12]*Edinburgh University, Edinburgh EH9 3JZ, United Kingdom*
[13]*Fairfield University, Fairfield, Connecticut 06824, USA*
[14]*Florida International University, Miami, Florida 33199, USA*
[15]*Florida State University, Tallahassee, Florida 32306, USA*
[16]*Università di Genova, 16146 Genova, Italy*
[17]*The George Washington University, Washington, D.C. 20052, USA*
[18]*The Hebrew University of Jerusalem, 91904, Israel*
[19]*Idaho State University, Pocatello, Idaho 83209, USA*
[20]*University of Illinois at Urbana-Champaign, Urbana, Illinois 61801, USA*
[21]*INFN, Sezione di Ferrara, 44100 Ferrara, Italy*
[22]*INFN, Laboratori Nazionali di Frascati, 00044 Frascati, Italy*
[23]*INFN, Sezione di Genova, 16146 Genova, Italy*

[24]INFN, Sezione di Roma Tor Vergata, 00133 Rome, Italy
[25]INFN, Gruppo collegato Sanità and Istituto Superiore di Sanità, Department TESA, I-00161 Rome, Italy
[26]Institut de Physique Nucléaire ORSAY, Orsay 91406, France
[27]Institute of Theoretical and Experimental Physics, Moscow, 117259, Russia
[28]James Madison University, Harrisonburg, Virginia 22807, USA
[29]Kent State University, Kent, Ohio 44242, USA
[30]University of Kentucky, Lexington, Kentucky 40506, USA
[31]Kyungpook National University, Daegu 702-701, Republic of Korea
[32]LPSC, Université Joseph Fourier, CNRS/IN2P3, INPG, Grenoble, France
[33]Massachusetts Institute of Technology, Cambridge, Massachusetts 02139, USA
[34]University of New Hampshire, Durham, New Hampshire 03824-3568, USA
[35]NRCN, P.O. Box 9001, Beer-Sheva 84190, Israel
[36]Norfolk State University, Norfolk, Virginia 23504, USA
[37]Ohio University, Athens, Ohio 45701, USA
[38]Old Dominion University, Norfolk, Virginia 23529, USA
[39]Rensselaer Polytechnic Institute, Troy, New York 12180-3590, USA
[40]Università di Roma Tor Vergata, 00133 Rome, Italy
[41]Rutgers, The State University of New Jersey, Piscataway, New Jersey 08855, USA
[42]Saint Mary's University, Halifax, Nova Scotia B3H 3C3, Canada
[43]Skobeltsyn Nuclear Physics Institute, 119899 Moscow, Russia
[44]University of South Carolina, Columbia, South Carolina 29208, USA
[45]Tel Aviv University, Tel Aviv 69978, Israel
[46]The University of Texas at Austin, Austin, Texas 78712, USA
[47]Temple University, Philadelphia, Pennsylvania 19122, USA
[48]Thomas Jefferson National Accelerator Facility, Newport News, Virginia 23606, USA
[49]Union College, Schenectady, New York 12308, USA
[50]Universidad Técnica Federico Santa María, Casilla 110-V Valparaíso, Chile
[51]University of Glasgow, Glasgow G12 8QQ, United Kingdom
[52]University of Virginia, Charlottesville, Virginia 22901, USA
[53]College of William and Mary, Williamsburg, Virginia 23187-8795, USA
[54]Yerevan Physics Institute, 375036 Yerevan, Armenia
(Received 21 March 2013; published 14 June 2013)

We have measured cross sections for the $\gamma^3\mathrm{He} \rightarrow pd$ reaction at photon energies of 0.4–1.4 GeV and a center-of-mass angle of 90°. We observe dimensional scaling above 0.7 GeV at this center-of-mass angle. This is the first observation of dimensional scaling in the photodisintegration of a nucleus heavier than the deuteron.

DOI: 10.1103/PhysRevLett.110.242301 PACS numbers: 25.20.−x, 21.45.−v, 24.85.+p

Dimensional scaling laws directly relate the energy dependence of the high-t (the four-momentum transfer squared) invariant cross sections to the number of constituents of the hadrons involved in the process. The origin of dimensional scaling is the scale invariance of the interactions among hadron constituents, and, thus, it naturally reflects the property of asymptotic freedom of QCD at small distance scales. The laws state that at fixed center-of-mass (c.m.) angle the cross section of an exclusive two-body-to-two-body nuclear reaction at large s (the total c.m. energy squared) and t is

$$\frac{d\sigma}{dt} \propto s^{2-n_i-n_f} = s^{-n}, \tag{1}$$

where n_i and n_f are the total number of elementary fields in the initial and final states that carry a finite fraction of particle momentum [1], e.g., 3 for a nucleon. Table I presents the experimental evidence for the success of these scaling laws.

Dimensional scaling is well founded and expected at asymptotic energies, where the available energy in the c.m. is much higher than the mass of the system. Under these circumstances, the only scale available is the energy and the s dependence arises from the norm of the active fields. However, data for many reactions show evidence for dimensional scaling even when s is roughly equal to the squared mass of the system, as is the case reported here.

To date there is no common model or theory that can describe all the data listed in Table I in a consistent manner. For processes on nuclear targets, phenomenological extensions of perturbative QCD (pQCD) based on factorization [18–20] have been developed and have shown limited success. A common feature of model interpretations of dimensional scaling, such as [1,21,22], is the dominance of a hard scattering mechanism in the reaction dynamics. It was, however, also discussed that soft QCD processes [23] or destructive interference among resonances [24] can mimic scaling at medium energies.

TABLE I. Selected hard exclusive hadronic and nuclear reactions that have been previously measured.

Reaction	s (GeV^2)	$\theta_{\text{c.m.}}$ (deg)	n Predicted	n Measured	Reference
$pp \to pp$	15–60	38–90	10	9.7 ± 0.5	[2]
$p\pi^- \to p\pi^-$	14–19	90	8	8.3 ± 0.3	[3]
$\gamma p \to \gamma p$	7–12	70–120	6	8.2 ± 0.5	[4]
$\gamma p \to \rho^0 p$	6–10	80–120	7	7.9 ± 0.3	[5]
$\gamma p \to p\pi^0$	8–10	90	7	7.6 ± 0.7	[6]
$\gamma p \to n\pi^+$	1–16	90	7	7.3 ± 0.4	[7]
$\gamma p \to K^+\Lambda$	5–8	84–120	7	7.1 ± 0.1	[8]
$\gamma d \to pn$	1–4	50–90	11	11.1 ± 0.3	[9–16]
$\gamma pp \to pp$	2–5	90	11	11.1 ± 0.1	[17]
$\gamma^3\text{He} \to pd$	11–15.5	90	17	17.0 ± 0.6	(This work)

From the standpoint of a nonperturbative approach, the scaling laws have been reviewed and derived using the AdS/CFT correspondence between string theories in anti–de Sitter space-time and conformal field theories in physical space-time [25]. Within this approach, the interactions between hadron constituents are scale invariant at very short but also at very large distances in the so-called "conformal window" where the effective strong coupling is large but constant, i.e., scale independent [26]. Thus, dimensional scaling laws may be probing the limits of two very different dynamical regimes of asymptotically large t and s, and of small t. In order to better understand the origin of scaling, we would need to also probe rigorously exclusive nuclear processes at very small t.

For reactions that are dominated by resonances, the study of scaling at smaller t is difficult since the resonances make it hard to determine whether scaling is observed. We chose to probe dimensional scaling in the reaction $\gamma^3\text{He} \to pd$ in the photon energy range 0.4–1.4 GeV. In this energy range, photoreactions on the proton and deuteron have shown signatures of scaling [7,9–16], but their interpretation is unclear. This reaction has the advantage that resonance mechanisms are suppressed (as shown by low-energy studies) [27]. In addition, there is evidence that two- and three-body mechanisms are important at large c.m. angles [28]; i.e., the momentum transfer is shared among two or three nucleons so that the average momentum transfer to each quark constituent would be small (maybe in the range of the conformal window). Our measurement is the first of this reaction in the GeV energy region. As previous measurements of photoinduced reactions have only involved $A = 1$ or 2, the expected quark-counting scaling power of $d\sigma/dt \propto s^{-17}$ is higher than any previous observation in photoproduction.

The data presented here were taken as part of Jefferson Lab (JLab) experiments 03-101 and 93-044, which ran at the continuous electron beam accelerator facility in Hall A [29] and in Hall B [30], respectively.

E03-101 was a measurement of the $\theta_{\text{c.m.}} = 90°$ energy dependence of the $^3\text{He}(\gamma, pp)n_{\text{spectator}}$ reaction [17]. In two kinematics at an incident electron energy of 1.656 GeV we could identify two-body photodisintegration of 3He into a proton and a deuteron at angles corresponding to $\theta_{p\,\text{c.m.}} = 85°$.

In this experiment, untagged bremsstrahlung photons were generated when the electron beam impinged on a copper radiator. The 6%-radiation-length radiator was located in the scattering chamber 38 cm upstream of the center of a 20-cm long cylindrical 0.079 g/cm^3 ^{3}He gas target. The size of the photon beam spot on the target, ≈ 2 mm, results from electron beam rastering intended to distribute the heat load across the target. The size of the target is much smaller than the $\approx$ 1-cm size of the target windows and apertures. Protons and deuterons from the target were detected in coincidence with the Hall-A high-resolution spectrometers [29]. The two spectrometers were set symmetrically on the two sides of the beam line in two kinematical settings corresponding to central momenta of 1.421 GeV/c at a scattering angle of 63.16° and 1.389 GeV/c at a scattering angle of 65.82°.

For each spectrometer, the scattering angles, momenta, and interaction positions at the target were reconstructed from trajectories measured with vertical drift chambers located in the focal plane. Two planes of plastic scintillators provided triggering and time-of-flight information for particle identification. Figure 1 shows the speed β of the two particles detected in coincidence. One clearly sees protons and deuterons in coincidence, with no visible backgrounds, such as pp and dd coincidences, or pions.

In analyzing the data from E03-101, the incident photon energy of the untagged beam was reconstructed event by event from the momentum and angles of the scattered particles under the assumption of two-body pd final-state kinematics. In order to assure the validity of this assumption and reduce backgrounds, the analysis is limited to events that fulfill two energy and momentum constraints: (1) $p_{T\text{missing}} \equiv p_{T(p)} + p_{T(d)} < 5\,\text{MeV}/c$, and (2) $\alpha_{\text{missing}} \equiv \alpha_d + \alpha_p - \alpha_{^3\text{He}} - \alpha_\gamma < 5 \times 10^{-3}$, where α is the light cone variable for each particle participating in the reaction

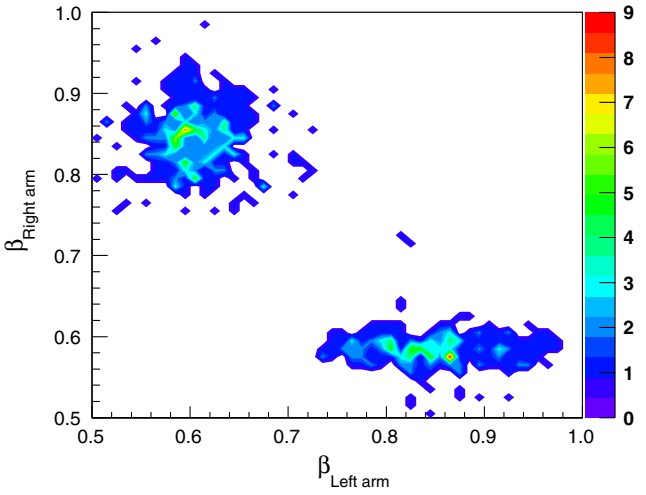

FIG. 1 (color online). The β distribution of particles detected in coincidence by the two high-resolution spectrometers in Hall A E03-101. The widths of the peaks result from the calibration and time resolution of the scintillators, from the momentum acceptance of the spectrometers ($\Delta p \approx \pm 3.5\%$), and the uncertainty of the path-length correction. The different scintillators in the two spectrometers lead to different widths of the distributions.

$$\alpha_X = A\frac{E^X - p_z^X}{E^A - p_z^A} \approx \frac{E^X - p_z^X}{m_A/A}, \tag{2}$$

where $A = 3$ is the mass number, E^X and p^X are, respectively, the energy and momentum of the particle, m_A, E^A, and p^A are the nucleus mass, energy, and momentum, respectively, and the z direction is the direction of the incident photon beam. With the above definitions, α_γ is zero, while $\alpha_{^3\mathrm{He}}$ is 3.

Simulations show that the inelastic processes present in the spectrum in Fig. 2 have negligible contribution to the cross section after the $p_{T\mathrm{missing}}$ and $\alpha_{\mathrm{missing}}$ cuts are applied.

The detected proton-deuteron pairs can result from either a photon or an electron disintegrating the ^{3}He nucleus. We took data with the radiator in and out of the beam, to extract the number of events resulting from photons produced in the bremsstrahlung radiator [13,17]. Event selection cuts on the target vertex and coincidence between the two spectrometers were applied using the same techniques as [17]. The finite acceptance correction was determined using the standard Hall-A Monte Carlo simulation software MCEEP [31].

The sources for the systematic uncertainties for E03-101 are described in [17]; for this analysis they are dominated by the finite acceptance correction, which is at the 4%–11% level.

Experiment E93-044 used the CEBAF large acceptance spectrometer (CLAS) to measure various photoproduction reactions on ^{3}He and ^{4}He targets. A collimated, tagged, real-photon beam was produced using the bremsstrahlung tagging facility in Hall B [32]. Photons with energies

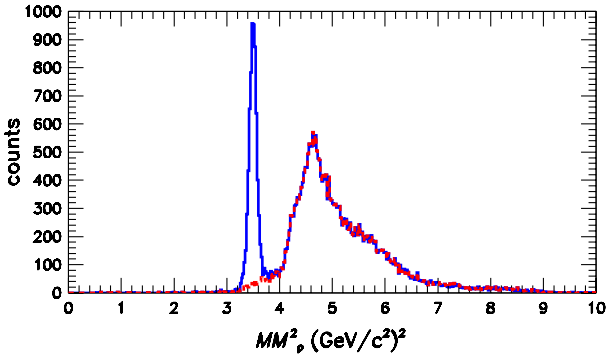

FIG. 2 (color online). Event distributions measured by CLAS, of the missing mass of the proton MM_p^2 for $\theta_{p\,\mathrm{c.m.}} = 90°$, with (dashed red line) and without (blue solid line) the kinematic cuts, are shown. Events from the pd final state are clearly identified in the peak. The background distribution (events rejected by the kinematic cuts) exhibits smooth behavior under the deuteron peak and reproduces the background shape outside of the peak.

between 0.35 and 1.55 GeV were incident on an 18-cm long cryogenic liquid ^{3}He target positioned in the center of CLAS. The outgoing protons and deuterons were tracked in the six toroidal magnetic spectrometers (sectors) of CLAS. Their trajectories were measured by three layers of drift chambers surrounding the target. Particle time of flight was measured by 6×57 scintillators enclosing CLAS outside of the magnetic field. CLAS covers a polar angular range from 8° to 142° and an azimuthal angular range from 0° to 360°, excluding the angles where the torus coils are located. More details about CLAS and experiment E93-044 can be found in [33,34], respectively.

In the analysis of data from E93-044, protons and deuterons were identified from momentum and time-of-flight measurements. Only events with one proton and one deuteron originating from the target were analyzed. Accidental and physics backgrounds were reduced by applying kinematic cuts making use of the constraints provided by two-body kinematics when both final-state particles are detected.

Figure 2 demonstrates the effect of the kinematic cuts on the proton missing-mass-squared, MM_p^2, distribution at $\theta_{p\mathrm{c.m.}} = 90°$. The proton missing mass squared is calculated as $MM_p^2 = (\tilde{p}_\gamma + \tilde{p}_{^3\mathrm{He}} - \tilde{p}_p)^2$, where $\tilde{p}_\gamma$, $\tilde{p}_{^3\mathrm{He}}$, and $\tilde{p}_p$ are the four-momenta of the beam, target, and detected final-state proton, respectively. The initial event distribution, before our kinematic cuts are applied, shows a well pronounced peak at around $3.5(\mathrm{GeV}/c^2)^2$ (which corresponds to the square of the deuteron mass), followed by a broader structure above $3.8(\mathrm{GeV}/c^2)^2$. While the peak contains predominantly the pd events of interest, the broader structure contains background produced in the reaction $\gamma\,^3\mathrm{He} \rightarrow pdX$, where X could be one or more missing particles. The low-mass tail of the background events extends under the pd peak. Our kinematic cuts select the good pd events from the initial sample and reject

background events. For simplicity, in Fig. 2 we show the events rejected by our kinematic cuts overlaid with the initial distribution. These background events exhibit smooth behavior under the deuteron peak and reproduce the background shape outside of the peak. The uncertainty of the yield extraction due to the remaining background events is $(2.30 \pm 0.63)\%$.

The CLAS acceptance for the reaction $\gamma^3\mathrm{He} \to pd$ was evaluated by generating 2×10^7 phase-space events and processing them through GSIM [35], a GEANT-3 program that simulates CLAS. The CLAS acceptance for pd events at a c.m. angle of 90° is $\approx 71\%$. The main contribution to the uncertainty of the CLAS acceptance is due to residual inefficiencies of various detector elements, such as scintillator paddles and drift-chamber wires. The uncertainty of the acceptance was evaluated by comparing our best estimate of acceptance to the acceptance of 100%-efficient CLAS, and by comparing the acceptance-corrected pd yields (real data) from each of the three independent CLAS spectrometers. All methods yielded that the systematic uncertainty of the CLAS acceptance is $<10\%$. The photon flux was calculated using the standard CLAS software [36] and has an uncertainty of 4.5% [37]. The uncertainty of the target length and density was 2% [34]. The total systematic uncertainty of the CLAS cross sections is $<11.4\%$, with the CLAS acceptance being the dominant source. The statistical uncertainties range from 2% to 40% depending on the energy bin. Full details about the analysis of the CLAS data will be given in a forthcoming long publication.

Figure 3 shows the resulting cross sections from CLAS and Hall A compared to previously published data [28] for $s > 10$ GeV^2. In the range of $s = 11.5$–15 GeV^2, the cross section falls by 2 orders of magnitude. The falloff of our Hall-A and CLAS data is fit as $s^{-17\pm0.6}$, which is consistent with the expected scaling degree of $n = 17$. This is the first observation of high-energy cross-section scaling for photodisintegration of an $A > 2$ system. We note that our data point at $s \approx 13.5$ GeV^2 is about 3.5 standard deviations below the scaling prediction. Because of the limited statistics in this kinematic bin, we cannot study in further detail whether the origin of this deviation is random or is due to physics.

Starting at threshold, the scaled invariant cross section, $s^{17}d\sigma/dt$, decreases smoothly to $E_\gamma = 0.7$ GeV where it levels out, a transition different from meson photoproduction [7] or pp breakup [17], where "resonancelike" structures are observed. Since our data are taken in the resonance region ($\sqrt{s} < 2$ GeV assuming a free nucleon target), this suggests that two- and three-nucleon mechanisms dominate the reaction dynamics or nucleon resonance contributions are strongly suppressed.

The scaled cross section of ≈ 30 Gb GeV^{32} corresponds to an invariant cross section of $d\sigma/dt \approx 0.4$ nb/GeV^2 for $E_\gamma \approx 1.3$ GeV. The corresponding cross section for $\gamma d \to pn$ at this energy is about 30 nb/GeV^2, about 2 orders of magnitude larger, while the cross section for $\gamma^3\mathrm{He} \to pp + n_{\mathrm{spectator}}$ at this energy is ≈ 13 nb/GeV^2, about 30 times larger. If one adopts the view that large momentum transfer reactions select initial states in which all the quarks and nucleons are close together, it is much more likely that there is a short-range, and thus high-momentum, pn pair than pp pair. This was observed in recent studies for nucleons above the Fermi surface that have momenta of several hundred MeV/c [38,39]. Furthermore, in ^{3}He there is nearly as large a probability for a short-range pd pair as for a pp pair [40].

The reduced nuclear amplitudes (RNA) prescription [18] was developed as a way of extending the applicability of pQCD to lower energy and momentum scales, by factoring out nonperturbative dynamics related to hadron structure through phenomenologically determined hadronic form factors. It should be noted that deuteron photodisintegration follows the dimensional scaling better than it follows the RNA prediction [15]. The RNA prescription for $\gamma^3\mathrm{He} \to pd$ is

$$\frac{d\sigma}{dt} \propto \frac{1}{(s - m^2_{^3\mathrm{He}})^2} F_p^2(\hat{t}_p) F_d^2(\hat{t}_d) \frac{1}{p_T^2} f^2(\theta_{\mathrm{c.m.}}). \quad (3)$$

Here, F_p (F_d) is the proton (deuteron) form factor, $\hat{t}_p$ ($\hat{t}_d$) is the momentum transfer to the proton (deuteron), and f is an unknown function of the c.m. angle that must be determined from experimental data. The overall normalization is also unknown, and ideally should be determined from data at asymptotically large momentum transfer. Figure 3 shows the RNA prediction, normalized to our highest energy data point from E03-101. Our data appear to agree better with dimensional scaling than with the RNA prediction.

The model of Laget [41] is an hadronic model based on a diagrammatic approach for the calculation of the dominant one-, two-, and three-body mechanisms contributing to the reaction. It provides good accounting of the absolute magnitude of the cross section and reproduces the scaling exhibited by the data over a limited energy range. Overall, the data appear to agree better with dimensional scaling than with the model.

We observe the onset of scaling at $\theta_{\mathrm{c.m.}} = 90°$ at a momentum transfer to the deuteron $|t| > 0.64\,(\mathrm{GeV}/c)^2$ and a transverse momentum $p_\perp > 0.95$ GeV/c. These momentum thresholds for scaling are remarkably low. For other processes, such as deuteron photodisintegration, the onset of scaling has been observed at $p_\perp > 1.1$ GeV/c [9–16]. Both the deuteron form factor and the reduced deuteron form factor [18] show scaling at $|t| > 2\,(\mathrm{GeV}/c)^2$. This comparison suggests that nonperturbative interpretation of our data may be more appropriate. Such interpretation in the framework of AdS/CFT means that the observed scaling is due to the near constancy of the effective QCD coupling at low Q (conformal window [26])

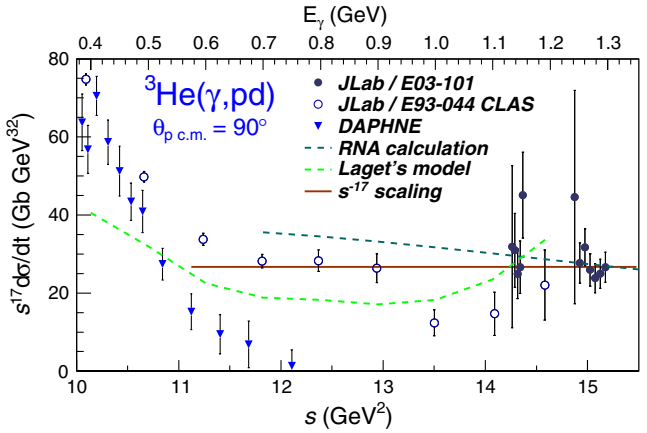

FIG. 3 (color online). The invariant cross section $d\sigma/dt$ multiplied by s^{17} to remove the expected energy dependence. The DAPHNE data are taken from [28]. The RNA [18] calculation is normalized to our highest energy data point from JLab E03-101. The prediction of Laget is based on a diagrammatic hadronic model [41]. Constant s^{17} scaling normalized to our highest energy data point is indicated by a solid red line. For a comment on the comparison between the CLAS and DAPHNE data, see [42].

and we are in the nonperturbative regime of QCD. A further test of this interpretation would require data over a higher-energy range where the transition from nonperturbative to perturbative dynamics would manifest itself in breaking dimensional scaling. The latter would be observed again at asymptotically large invariants when pQCD sets in.

Our result indicates that QCD studies of nuclei are meaningful at energies as low as $E_\gamma = 0.7$ GeV and that the three-nucleon bound system may be an equally good laboratory for such studies as the deuteron. Moreover, since the cross section for our process had been previously measured down to beam energies of a few MeV, our data combined with the low-energy data allow us to map for the first time the transition from meson-nucleon to partonic degrees of freedom cleanly, without the complication of resonance structures, as has been the case in previous studies involving $A = 1$ or $A = 2$ nuclear systems.

We have observed for the first time scaling in an exclusive reaction initiated by a photon beam and involving an $A = 3$ nucleus. The scaling power of s^{-17} for $E_\gamma > 0.7$ GeV is the highest quark-counting power-law dependence observed to date in leptoproduction. If AdS/CFT correspondence is the proper framework to understand the origin of dimensional scaling, then the observed scaling is a result of the near constancy of the QCD coupling. This assumption may be validated through the study of this reaction in a higher-energy range.

We thank S. J. Brodsky, L. L. Frankfurt, M. M. Sargsian, and M. Strikman for helpful discussions. We thank the JLab physics and accelerator divisions for their support. This work was supported in part by the U.S. National Science Foundation under Grant No. PHY-0856010, the U.S. Department of Energy, the Israel Science Foundation, the U.S.-Israeli Bi-National Scientific Foundation, the Chilean Comisión Nacional de Investigación Científica y Tecnológica (CONICYT), the Istituto Nazionale di Fisica Nucleare, the French Centre National de la Recherche Scientifique, the French Commissariat à l'Energie Atomique, the UK Science and Technology Facilities Council (STFC), the Scottish Universities Physics Alliance (SUPA), and the National Research Foundation of Korea. Jefferson Science Associates operates the Thomas Jefferson National Accelerator Facility under DOE Contract No. DE-AC05-06OR23177.

*Deceased
†Present address: Skobeltsyn Nuclear Physics Institute, 119899 Moscow, Russia.
‡Present address: Institut de Physique Nucléaire ORSAY, Orsay, France.
§Present address: INFN, Sezione di Genova, 16146 Genova, Italy.
‖Present address: Università di Roma Tor Vergata, 00133 Rome, Italy.

[1] S. J. Brodsky and G. R. Farrar, Phys. Rev. Lett. **31**, 1153 (1973).
[2] A. W. Hendry, Phys. Rev. D **10**, 2300 (1974).
[3] K. A. Jenkins, L. Price, R. Klem, R. Miller, P. Schreiner, M. Marshak, E. Peterson, and K. Ruddick, Phys. Rev. D **21**, 2445 (1980).
[4] A. Danagoulian *et al.*, Phys. Rev. Lett. **98**, 152001 (2007).
[5] M. Battaglieri *et al.*, Phys. Rev. Lett. **87**, 172002 (2001).
[6] D. G. Meekins *et al.*, Phys. Rev. C **60**, 052201 (1999).
[7] L. Y. Zhu *et al.*, Phys. Rev. Lett. **91**, 022003 (2003).
[8] R. A. Schumacher and M. M. Sargsian, Phys. Rev. C **83**, 025207 (2011).
[9] J. Napolitano *et al.*, Phys. Rev. Lett. **61**, 2530 (1988).
[10] S. J. Freedman *et al.*, Phys. Rev. C **48**, 1864 (1993).
[11] J. E. Belz *et al.*, Phys. Rev. Lett. **74**, 646 (1995).
[12] C. Bochna *et al.*, Phys. Rev. Lett. **81**, 4576 (1998).
[13] E. C. Schulte *et al.*, Phys. Rev. Lett. **87**, 102302 (2001).
[14] E. C. Schulte *et al.*, Phys. Rev. C **66**, 042201 (2002).
[15] M. Mirazita *et al.*, Phys. Rev. C **70**, 014005 (2004).
[16] P. Rossi *et al.*, Phys. Rev. Lett. **94**, 012301 (2005).
[17] I. Pomerantz *et al.*, Phys. Lett. B **684**, 106 (2010).
[18] S. J. Brodsky and J. R. Hiller, Phys. Rev. C **28**, 475 (1983).
[19] L. L. Frankfurt, G. A. Miller, M. M. Sargsian, and M. I. Strikman, Phys. Rev. Lett. **84**, 3045 (2000).
[20] M. M. Sargsian and C. Granados, Phys. Rev. C **80**, 014612 (2009).
[21] V. A. Matveev, R. M. Muradian, and A. N. Tavkhelidze, Nuovo Cimento Lett. **7**, 719 (1973).
[22] X. Ji, J.-P. Ma, and F. Yuan, Phys. Rev. Lett. **90**, 241601 (2003).
[23] A. V. Radyushkin, Phys. Lett. B **642**, 459 (2006).

[24] Q. Zhao and F. E. Close, Phys. Rev. Lett. **91**, 022004 (2003).
[25] J. Polchinski and M. J. Strassler, Phys. Rev. Lett. **88**, 031601 (2002).
[26] S. J. Brodsky and G. F. de Téramond, Phys. Rev. D **77**, 056007 (2008).
[27] P. Picozza, C. Schaerf, R. Scrimaglio, G. Goggi, A. Piazzoli, and D. Scannicchio, Nucl. Phys. A **157**, 190 (1970).
[28] V. Isbert *et al.*, Nucl. Phys. A **578**, 525 (1994).
[29] J. Alcorn *et al.*, Nucl. Instrum. Methods Phys. Res., Sect. A **522**, 294 (2004).
[30] B. L. Berman, G. Audit, and P. Corvisiero, "Photoreactions on ^{3}He," Jefferson Lab Experiment E93-044, 1993.
[31] P. E. Ulmer, Jefferson Lab Report No. CEBAF-TN-91-101, 1991.
[32] D. I. Sober *et al.*, Nucl. Instrum. Methods Phys. Res., Sect. A **440**, 263 (2000).
[33] B. A. Mecking *et al.*, Nucl. Instrum. Methods Phys. Res., Sect. A **503**, 513 (2003).
[34] S. Niccolai *et al.*, Phys. Rev. C **70**, 064003 (2004).
[35] GSIM, CLAS Simulation Software, 1997.
[36] J. Ball and E. Pasyuk, CLAS Note No. 2005-002, 2005, https://misportal.jlab.org/ul/Physics/Hall-B/clas/viewFile.cfm/2005-002.pdf?documentId=24.
[37] Y. Ilieva *et al.*, Eur. Phys. J. A **43**, 261 (2010).
[38] R. Subedi *et al.*, Science **320**, 1476 (2008).
[39] R. Shneor *et al.*, Phys. Rev. Lett. **99**, 072501 (2007).
[40] M. M. Sargsian, T. V. Abrahamyan, M. I. Strikman, and L. L. Frankfurt, Phys. Rev. C **71**, 044615 (2005).
[41] J. M. Laget, Phys. Rev. C **38**, 2993 (1988).
[42] At this time, the disagreement between the CLAS and DAPHNE data at $E_\gamma > 0.5$ GeV is not well understood. The DAPHNE yields were corrected by a factor of up to 42% depending on photon energy and c.m. angle. Their analysis is more reliable at kinematics where the final state particles stop in the detector. The largest disagreement between the two data sets is at mid c.m. angles where both the proton and the deuteron have large momenta and do not stop in the DAPHNE detector. This may lead to a large systematic uncertainty in their correction factor. A comparison of the CLAS and DAPHNE data sets for a wider angular range is in preparation.